

# Dalton Transactions

Accepted Manuscript



This is an *Accepted Manuscript*, which has been through the Royal Society of Chemistry peer review process and has been accepted for publication.

*Accepted Manuscripts* are published online shortly after acceptance, before technical editing, formatting and proof reading. Using this free service, authors can make their results available to the community, in citable form, before we publish the edited article. We will replace this *Accepted Manuscript* with the edited and formatted *Advance Article* as soon as it is available.

You can find more information about *Accepted Manuscripts* in the [Information for Authors](#).

Please note that technical editing may introduce minor changes to the text and/or graphics, which may alter content. The journal's standard [Terms & Conditions](#) and the [Ethical guidelines](#) still apply. In no event shall the Royal Society of Chemistry be held responsible for any errors or omissions in this *Accepted Manuscript* or any consequences arising from the use of any information it contains.

# All High-Spin ( $S = 2$ ) Iron(II) Hemes are NOT Alike

Chuanjiang Hu,<sup>\*,†</sup> Charles E. Schulz,<sup>\*,‡</sup> and W. Robert Scheidt<sup>\*,§</sup>

Contribution from Key Laboratory of Organic Synthesis  
of Jiangsu Province, College of Chemistry, Chemical Engineering  
and Materials Science, Soochow University, Suzhou 215123, P.R. China,  
Department of Physics, Knox College, Galesburg, Illinois 61401, USA,  
and Department of Chemistry and Biochemistry,  
University of Notre Dame, Notre Dame, Indiana 46556, USA

September 5, 2015

## Corresponding Authors

E-mail: cjhu@suda.edu.cn

E-mail: cschulz@knox.edu

E-mail: scheidt.1@nd.edu

---

<sup>†</sup>Soochow University

<sup>‡</sup>Knox College

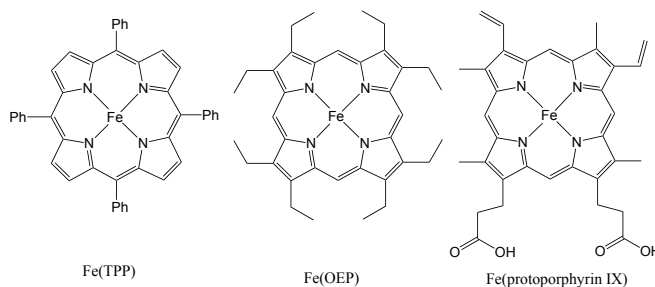
<sup>§</sup>University of Notre Dame

ABSTRACT: A common structural motif in heme proteins is a five-coordinate species in which the iron is coordinated by a histidyl residue. The widely distributed heme proteins with this motif are essential for the well being of humans and other organisms. We detail the differences in molecular structures and physical properties of high-spin iron(II) porphyrin derivatives ligated by neutral imidazole, hydrogen bonded imidazole, and imidazolate or other anions. Two distinct (high spin) electronic states are observed that have differing d-orbital occupancies and discernibly different five-coordinate square-pyramidal coordination groups. The doubly occupied orbital in the imidazole species is a low symmetry orbital oblique to the heme plane whereas in the imidazolate species the doubly occupied orbital is a high symmetry orbital in the heme plane, i.e., the primary doubly-occupied d-orbital is different. Methods that can be used to classify a particular complex into one or the other state includes X-ray structure determinations, high-field Mössbauer spectroscopy, vibrational spectroscopy, magnetic circular dichroism, and even-spin EPR spectroscopy. The possible functional significance of the ground state differences has not been established for heme proteins, but is likely found in the pathways for oxygen transport vs. oxygen utilization.

## I. INTRODUCTION

Heme proteins carry out a wide range of physiological functions using the same prosthetic group, iron protoporphyrin IX; a large number of these hemoproteins are important for human health. A common structural motif is the coordination of a single axial histidine, usually called the proximal ligand, to form high-spin five-coordinate species. Functions carried out by heme proteins with this structural motif include oxygen transport and storage, oxygen utilization and oxidations in the peroxidases, dioxygenases, cyclooxygenases, and heme catabolism (heme oxygenase), NO reductases, NO signaling, and NO transport, to name some important systems. Control of the heme environment is one path to accomplishing this variety of functions. Hydrogen bonding to the histidine has long been suggested as an important component<sup>1, 2</sup> and weak hydrogen bonds are found in the crystal structures of the globins but strong hydrogen bonds in the peroxidases.<sup>3, 4</sup>

In this Perspective, we describe our characterization of high-spin iron(II) porphyrinates ligated by imidazole species. Scheme 1 illustrates the framework of three important iron(II) porphyrinates and Figure 1 shows a schematic of the five-coordinate imidazole complex. Their complete description requires recognizing two distinct electronic states; these have distinctly different orbital symmetries. High-spin iron(II) porphyrinates ( $S = 2$ ) should, in principle, be easy to describe. The  $d^6$  configuration and square-pyramidal geometry means that the electronic configuration can be specified by which one of the three d-orbital  $d_{xy}$ ,  $d_{xz}$ , or  $d_{yz}$  is the doubly occupied one.



**Scheme 1.** Diagrams of three important four-coordinate iron(II) porphyrinates.

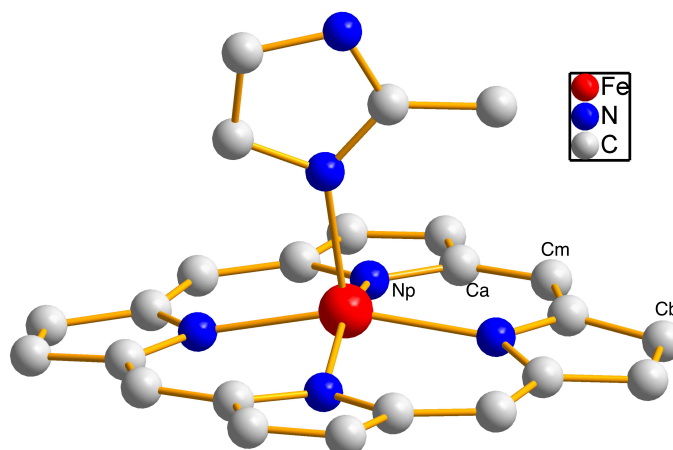


**Figure 1.** Diagram of 2-methylimidazole coordinated to an iron porphyrinate. The two Fe–N<sub>p</sub> bonds to the right (closest) to the axial ligand are typically slightly shorter than the other two Fe–N<sub>p</sub> bonds. Atom types are labeled: N<sub>p</sub>, porphyrin nitrogen atoms, C<sub>a</sub>,  $\alpha$  carbon atoms, C<sub>m</sub>, methine carbon atoms, C<sub>b</sub>,  $\beta$  carbon atoms.

The preparation of five-coordinate high-spin iron(II) porphyrinates requires appropriate precursors, the most useful are four-coordinate iron(II) porphyrinates. Since most iron porphyrinate systems have the stable oxidation state of 3+, reduction, preferably one that yields four-coordinate species, is required. Three useful methods are: inner electron transfer,<sup>5</sup> zinc amalgam,<sup>6</sup> or ethanethiol reduction.<sup>7</sup> We have found the last procedure to be general and most convenient for preparing four-coordinate species.

## II. IMIDAZOLE LIGANDS

The five-coordinate iron(II) porphyrinate, [Fe(TPP)(2-MeHIm)] reported by Collman and Reed,<sup>5</sup> was the first synthetic model for the deoxy site of myoglobin and hemoglobin.<sup>8</sup> The sterically demanding 2-methylimidazole inhibits the addition of a sixth ligand and a low-spin state, while still yielding an unconstrained five-coordinate complex. The X-ray structure was determined in the laboratory of J.L. Hoard and first results were reported at a National ACS meeting.<sup>9</sup> Complete results were never published, but some of the metrical data was published in a Scheidt/Hoard PNAS article.<sup>10</sup> Prof. Hoard also gave one of us (WRS) the complete set of atomic coordinates and other details. A notable structural feature was the substantial C<sub>4v</sub> doming of the porphyrin core described by the large (0.13 Å) separation between the plane of the four nitrogen atoms and the 24-atom mean plane. In an idealized C<sub>4v</sub> domed core, the iron

is displaced above the plane of the four nitrogen atoms with the planes of the eight  $C_a$  carbons, the four methine carbon atoms and the eight  $C_b$  carbons successively further below (see Figure 1 for atom naming). A common quantitative measure of doming is the perpendicular distance between the four nitrogen plane and the average plane of all 24 atoms of the porphyrin ring. The Fe–N<sub>p</sub> bond distances (2.086(8) Å) are longer than those found for the five-coordinate iron(III) species. The iron(II) center is displaced by 0.42 Å from the N<sub>4</sub> plane; all features are consistent with the expected large size of high-spin iron(II). These structural features were long assumed to be typical of high-spin iron(II) coordinated to the porphyrin ligand. In their 1981 review of spin state/stereochemical relationships,<sup>11</sup> Scheidt and Reed described all high-spin iron(II) species as having the  $(d_{xy})^2(d_{xz},d_{yz})^2(d_{z^2})^1(d_{x^2-y^2})^1$  configuration, consistent with the large displacement of iron in the five-coordinate species. It is now clear that the configuration assignment and other assumptions must be more complex; this Perspective traces our path towards a better understanding of high-spin iron(II) hemes, which began with the unanticipated result below.

In the course of other studies we obtained a second crystalline form of [Fe(TPP)(2-MeHIm)];<sup>12</sup> this unexpected new phase intrigued us sufficiently to carry out detailed characterization.<sup>13</sup> During the initial X-ray structure determination, it was clear that for this form, unlike the earlier form, crystallographic disorder of the axial ligand was not required. The structure determination further revealed that iron(II) porphyrinates display substantial structural pliability with variations in core conformation, iron atom displacements, porphyrin core hole size, and axial and equatorial Fe–N bond distances. The almost completely ordered axial imidazole is tilted off-axis because of the bulky 2-methyl substituent. This leads to a small asymmetry in the equatorial Fe–N<sub>p</sub> distances with the two equatorial bonds closer to the ligand shorter than the other two. The different core conformation of the two forms led us to synthesize and characterize several additional tetraarylporphyrin derivatives that further demonstrated the structural diversity;<sup>14</sup> the then commonly held view that only domed cores would be observed for high-spin iron(II) is clearly incorrect.

We also characterized two octaethylporphyrinato derivatives,  $[\text{Fe}(\text{OEP})(2\text{-MeHIm})]$  and  $[\text{Fe}(\text{OEP})(1,2\text{-Me}_2\text{Im})]$ ; only one has a moderately domed core.<sup>15</sup> A final derivative, a modified picket fence porphyrin,  $[\text{Fe}(\text{Piv}_2\text{C}_8)((1\text{-MeIm})]$ , has an unhindered axial imidazole.<sup>16</sup> But the necessary straps and pickets needed to block one face of the porphyrin lead to a severely constrained and saddled core. Thus, the core conformations are widely variable as seen in Figure 2, and core-domed species are not dominant. The displacement of the iron center from

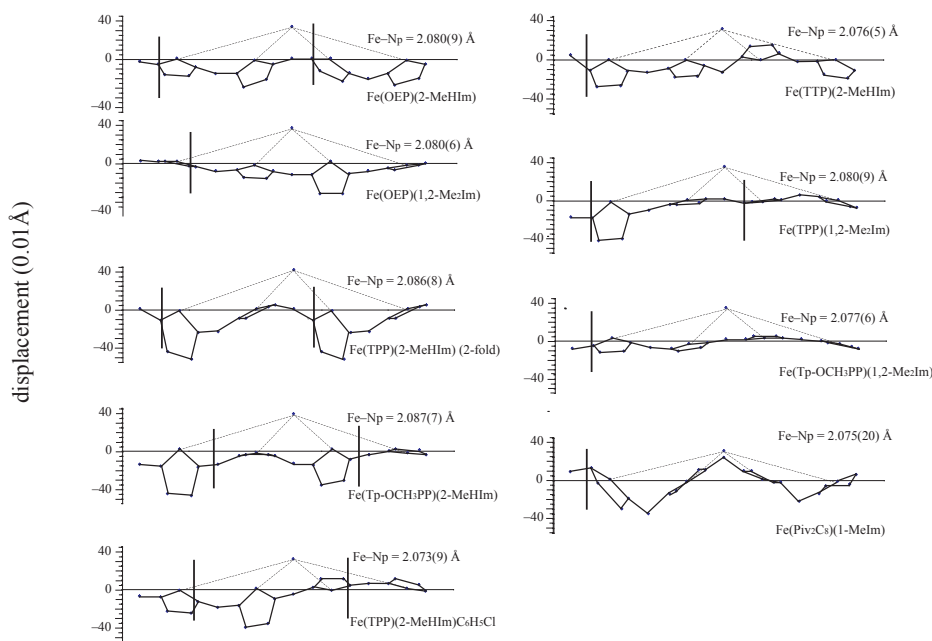


**Figure 2.** “Shoestring” diagrams illustrating the core conformation and iron displacement for nine known imidazole-ligated high-spin iron(II) porphyrinates. The mean plane defined by the four porphyrin nitrogens is the horizontal line and the cyclic porphyrin molecule is displayed in a linear fashion. The perpendicular displacement of the iron and other atoms of the core are shown from this four nitrogen plane. Bonds from the iron to the nitrogens are shown and the position of the imidazole ligand with respect to directions defined by the  $\text{Fe-N}_p$  directions is shown by the vertical line (or lines when the imidazole has two positions).

the  $\text{N}_4$  plane rather than the full 24-atom mean plane is the more appropriate measure of the out-of-plane displacement of iron because the varying core conformations lead to large variance in the latter.

At this point, a total of nine different five-coordinate high-spin imidazole-ligated porphyrin derivatives had been structurally characterized: seven with tetraarylporphyrins and two with

octaethylporphyrin. The structural parameters for these are found to be very tightly clustered. A complete listing of individual values can be found in Table 3 of Ref. 15 and we provide only a summary here. In all values that follow, the number in parentheses following the averaged value is the estimated standard deviation (esd) calculated on the assumption that all values are drawn from the same population. The average distance from the iron to the porphyrin nitrogens ( $N_p$ ) is 2.080 (5) Å, and the distance to the axial ligand is 2.147 (16) Å. The displacement of iron from the  $N_4$  plane cluster around 0.36 (3) Å, whereas the displacement from the 24 atom plane is larger with more variability at 0.44 (6) Å. A final parameter of interest is the off-axis tilt of the Fe–N(Im) vector from the normal to the heme plane, which is 7.8 (24)°. The off-axis tilt is the result of the bulky 2-substituent of all imidazoles with variability the result of core conformation differences.

Along with detailed structure determinations, we sought to fully characterize the electronic structure of these new derivatives. Many of the spectroscopic probes useful for iron(III) derivatives are not useful for iron(II). One probe that does provide substantial information is Mössbauer spectroscopy. We have carried out measurements on many species in high magnetic field (up to 9T) and over a wide range of temperatures. The quadrupole splitting constants ( $\Delta E_q$ ) range from 1.93 to 2.44 mm/s with isomer shifts of 0.86 to 0.95 mm/s and relatively large values of the asymmetry parameter  $\eta$ . These values are wholly consistent with earlier high field measurements of Lang and coworkers<sup>17, 18</sup> on deoxymyoglobin and deoxyhemoglobin and on two small molecule species prepared by Reed and Collman.<sup>5</sup> Importantly, the high field spectra allows the determination of the sign of electric field gradients and the quadrupole splitting constant, which is negative. Equally important, the maximum electric field gradient component is not along the heme normal, but oblique to it. In other words, the electronic structure is one of low symmetry.

We have tabulated Mössbauer study values for the high-spin iron(II) porphyrinates in Table 1, that we place at the end of the Perspective. We give for all possible species, the signed value of the quadrupole splitting, the isomer shift, and the asymmetry parameter,  $\eta$ .



Although there are modest differences in detail, all  $\Delta E_q$  values show a significant T-dependence with decreasing values as the temperature is increased. This is the result of low-lying excited states of the same or lower spin multiplicity (within  $\sim 300 \text{ cm}^{-1}$ ) above the ground state for all species, both protein and small molecule. One parameter that did show variation was the zero field splitting parameter. Although the experimental uncertainties of the determination of the zero field splitting by Mössbauer spectroscopy are large, it seems certain that the sign can be either + or - with some range in the values as well. This suggests that the ground state in all species is not exactly the same, but is sensitive to small variations in structure, including variation in core conformation and core doming, axial ligand tilting, and axial ligand orientation. This sensitivity of the crystal field parameters to small structural changes is supported by DFT calculations which showed that the energy minimized structure and the experimentally observed structure yield zero field splitting values differing in sign.<sup>19</sup> Most of the Mössbauer spectra in high field show diffuse features including both deoxyMb and -Hb. Sharp spectra were observed for [Fe(TPP)(2-MeHIm)] and to a lesser extent for [Fe(OEP)(2-MeHIm)] and [Fe(OEP)(1,2-Me<sub>2</sub>Im)]. Nonetheless, the negative sign of the quadrupole splitting, similar large values of the asymmetry parameter,  $\eta$ , and isomer shifts do require that the basic features of the low-symmetry, doubly occupied *d* orbital are similar in deoxymyoglobin, deoxyhemoglobin, and all the imidazole-ligated synthetic models.

Two pyrazole-ligated iron(II) derivatives were also characterized, [Fe(TPP)(Hdmpz)] and [Fe(TpOCH<sub>3</sub>PP)(Hdmpz)].<sup>20</sup> The change in the axial nitrogen ligand does not lead to significant differences in either the molecular or electronic structure compared to the imidazole derivatives as shown by X-ray and Mössbauer studies.

### III. ANIONIC LIGANDS

There are, interestingly enough, several high-spin iron(II) derivatives that are distinctly different from the N-ligated species. These are porphyrinates in which the iron(II) is coordinated to an axial anionic ligand such as a halide or an anionic oxygen ligand.<sup>21–29</sup> These species have coordination group geometries in which all structural features that are expected to be sensitive

to the “size” of the central iron have values consistent with a larger iron(II) center compared to the imidazole-ligated complexes.

A comparison is shown in Figure 3. The structural and other physical properties of the two classes are seen to be substantially different but the origins of the differences between the two

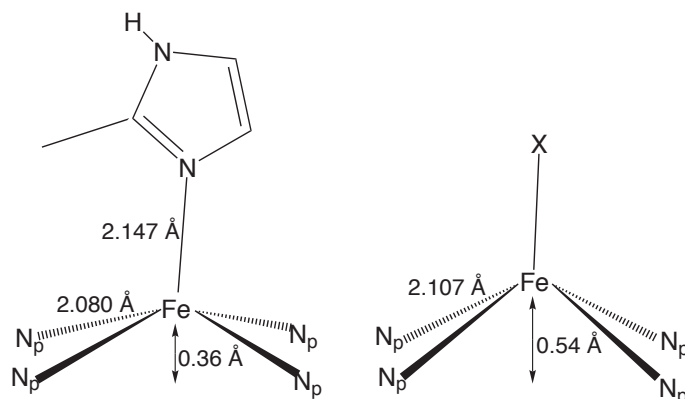


**Figure 3.** Diagrams illustrating the structural differences between high-spin iron porphyrinates coordinated to imidazole vs. axial anions (right). The number to the left in each diagram is the average Fe–N<sub>p</sub> distance, the middle number is the iron displacement from the four nitrogen plane and the top number is the value of the axial bond distance.

was not originally completely elucidated. A key observation is found in the Mössbauer spectra. The magnitude of the quadrupole splitting was immediately noted as being extremely large (>4 mm/s) and comparable to that seen in cytochrome P460 (hydroxylamine oxidase).<sup>30</sup> The  $\Delta E_q$  values are temperature independent indicating a well-isolated ground state. Values of the isomer shift were seen to be modestly larger than those of the imidazoles.

A key study was by Lang and coworkers<sup>25</sup> who carried out high field Mössbauer measurements on the phenoxide derivative,  $[\text{Fe}(\text{TPP})(\text{OC}_6\text{H}_5)]^-$ . This study showed that this class of high-spin iron(II) derivatives not only had much higher values of the quadrupole splitting, but the sign was positive with an asymmetry parameter of  $\sim 0$ . The sign of  $\Delta E_q$  is only available from high field measurements. Importantly, as the review by Debrunner<sup>31</sup> illustrates, the sign of  $\Delta E_q$  provides important information about d-orbital occupation. For high-spin  $d^6$  iron, only the doubly occupied  $d_{xy}$  or  $d_{x^2-y^2}$  orbital leads to a positive value, all other d-orbitals lead to negative values of  $\Delta E_q$ . Thus this positive sign of  $\Delta E_q$  must result from the doubly occupied

orbital being a high symmetry orbital, namely the  $d_{xy}$  orbital. This analysis was confirmed by two additional studies.<sup>27, 29</sup> The nature of the low-symmetry orbital of the imidazole derivatives is very different from that of a doubly occupied  $d_{xy}$  orbital and will be further discussed shortly.

The differences between the imidazole derivatives and halide or oxygen anionic species suggest that converting imidazole to an anionic imidazolate would lead to new species having interesting properties. This question was partly answered by a study of Mandon et al.<sup>32</sup> who prepared a picket fence porphyrin derivative with imidazolate as the sole axial ligand. In addition to a crystal structure, a zero-field Mössbauer study showed a relatively large quadrupole split doublet of 3.51 mm/s at 77 K. The sign of  $\Delta E_q$  was not defined in this study. In a later study, Hu et al.<sup>33</sup> reported the structures and high-field Mössbauer characterization of two imidazolate derivatives,  $[\text{Fe}(\text{TPP})(2\text{-MeIm}^-)]^-$  and  $[\text{Fe}(\text{OEP})(2\text{-MeIm}^-)]^-$ , the values of  $\Delta E_q$  were +3.60 and +3.71 mm/s, respectively, with a modest temperature-dependent change in the quadrupole splitting. The structures of the five-coordinate imidazolate species were quite different from that of the imidazoles. The Fe–N<sub>p</sub> bond distances and iron atom displacement are significantly larger in the imidazolate species while the axial bond is substantially shorter. A comparison of the coordination group geometries of imidazoles vs. imidazolates is given in Figure 4. Thus the removal of the N–H proton of imidazole leads to dramatic change in both the molecular and electronic structure of the five-coordinate high-spin iron(II) complex.

#### IV. DISTINGUISHING THE TWO STATES

The large structural differences between the imidazole and imidazolate shown in Figure 4 should be readily observed in the vibrational spectra. Nuclear resonance vibrational spectroscopy<sup>34</sup> measurements have been carried out for both imidazole<sup>35</sup> and imidazolate<sup>36</sup> species. Oriented crystal spectra for  $[\text{Fe}(\text{TPP})(2\text{-MeHIm})]$  and  $[\text{Fe}(\text{OEP})(2\text{-MeHIm})]$  could be measured in two orthogonal directions, but only in-plane spectra could be measured for the corresponding imidazolates. However, this provides sufficient information to allow for a confident assessment of the vibrational differences. As expected, the in-plane motions of iron are shifted to lower frequency in the imidazolate derivatives. A single out-of-plane mode with simultaneous iron

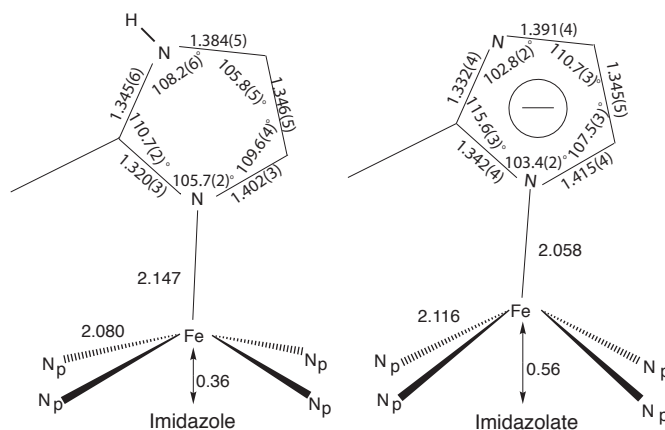


**Figure 4.** Diagram illustrating the differences in the coordination group structure and the five-membered ring geometry between imidazole and imidazolate species. The number to the left in each diagram is the average Fe–N<sub>p</sub> distance, the middle number is the iron displacement from the four nitrogen plane and the top number is the value of the axial bond distance. Distances and angles for the ligand ring are also displayed.

and imidazole(ate) motion is found in the two sets of complexes. The imidazolate derivatives display higher frequencies than the analogous imidazoles consistent with the shorter axial bond. Thus the general pattern of vibrations of the imidazoles and imidazolates are very similar, but with substantial differences in the frequencies that accurately reflect bond distance differences.

To summarize, both the Mössbauer spectra and the molecular structures clearly show that the anionic species including the imidazolates have a high symmetry doubly occupied orbital ( $d_{xy}$ ) whereas the imidazoles have a low symmetry doubly occupied orbital. Can these two states of high-spin iron(II) be distinguished in other ways? We describe other methods that have been successfully used in the following sections.

We explored the application of even-spin electron paramagnetic resonance (EPR), variable magnetic field and variable temperature magnetic circular dichroism spectroscopy (MCD) and DFT calculations to distinguish the two classes.<sup>19</sup> Although the imidazole and imidazolate derivatives both show  $g$ -values at  $\sim 9$ , the differences in the even spin EPR are consistent with large differences in the value of  $D$  and probably the sign of  $D$ . There are also differences in the T-dependent spectra (2–30K) that clearly show that the two systems have different electronic states. See Ref 19 for further details.

Magnetic circular dichroism (MCD) spectra have also been found to be useful. The MCD distinctions for the two electronic structures are found in substantial differences in the absolute molar **C**-term intensities that should allow for clear distinctions to be made and has, in addition, the advantage of requiring small amounts of material.

DFT calculations have been used to obtain fully optimized structures for both [Fe(TPP)(2-MeHIm)] and [Fe(TPP)(2-MeIm<sup>-</sup>)]<sup>-</sup> using BP86/TZVP without any simplifications. Good agreement between the experimental and predicted molecular structures was obtained with excellent predictions for the differences in the values of Fe-N<sub>p</sub>, Fe-N(Im), and the iron  $\Delta N_4$  out-of-plane displacement.

The key test of DFT is the correct prediction of the physical parameters that distinguish the two electronic states, in particular, the sign of  $\Delta E_q$  and the asymmetry parameter,  $\eta$ . Calculations using the optimized structures of [Fe(TPP)(2-MeHIm)] and [Fe(TPP)(2-MeIm<sup>-</sup>)]<sup>-</sup> with either BP86/TZVP or BP86/TZVP + CP(PPP) predict the correct signs of  $\Delta E_q$  and the qualitative values of  $\eta$ . Interestingly, using the experimental structural values rather than the optimized structures (although the differences are small) also improved the agreement of  $\eta$  and now gave the correct signs for the zero field splitting constants  $D$ . The latter suggests that small differences in structures are especially significant for the calculation of the excited state energies. However, the importance of the choice of functionals for DFT predictions is shown by calculations with B3LYP/TZVP (with CP(PPP) on iron). These calculation failed to predict the differing signs of  $\Delta E_q$  for the two states.

These BP86 calculations have also provided insight into the nature of the two electronic states. Given the strong accord of the DFT results with the Mössbauer results, we believe that the two methods combined represent the best description available.<sup>19</sup> For the imidazole complexes, the highest *doubly* occupied MO is based on a doubly occupied  $d_{xz}$  orbital in the plane of the imidazole. This MO is strongly mixed with a porphyrin  $E_{(g)}$  orbital with the final MO having 65%  $d_{xz}$  character. The Mössbauer results, from the determination of the electric field gradient (EFG), requires that this orbital to be oblique to the heme plane. This is possible

because the MO is not a pure  $d_{xz}$  orbital. The energy of the singly occupied  $d_{yz}$  orbital is about  $2200\text{ cm}^{-1}$  above  $d_{xz}$ , with the  $d_{xy}$  orbital higher still. A qualitative diagram showing the d-orbital energy ordering is given on the left-hand side of Figure 5.

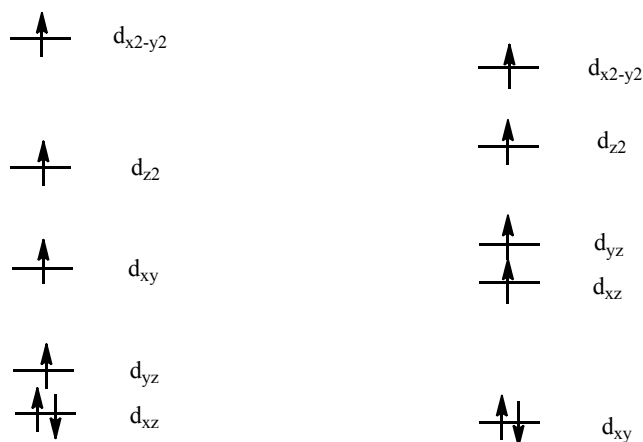


**Figure 5.** Diagram illustrating the approximate d-orbital energies for the two distinct states of high-spin iron(II) hemes. The diagram on the left-hand side is that for imidazole derivatives, whereas that on the right is for the imidazoles and other anions. Note that the doubly occupied orbital for both, but especially that for the imidazoles, is not a pure d-orbital but has significant porphyrin orbital character.

For the imidazolate species, the *doubly* occupied MO has as its principal component the  $d_{xy}$  orbital, which is parallel to and in the porphyrin plane. The population of this orbital is consistent with the larger displacement of iron out-of-plane in the anionic species, along with the longer Fe–N<sub>p</sub> bond distance compared to the imidazole derivatives. The  $\pi$ -donation of the imidazolate pushes up the energy of the singly occupied  $d_{yz}$  orbital and both it and the  $d_{xz}$  are much higher in energy than the  $d_{xy}$ . A qualitative d-orbital energy ordering is given on the right-hand side of Figure 5. Figure 6 provides DFT-calculated frontier orbitals for the two distinct systems.

## V. HYDROGEN BONDING EFFECTS

Although there have been many Mössbauer studies of globins (hemoglobin and myoglobin), to our knowledge there is only a single study of a peroxidase (horseradish peroxidase, HRP), which in the reduced iron(II) state is five-coordinate with a histidyl axial ligand. The study of Champion et al.<sup>37</sup> found the isomer shift to be  $0.90\text{ mm/s}$  and the quadrupole splitting constant

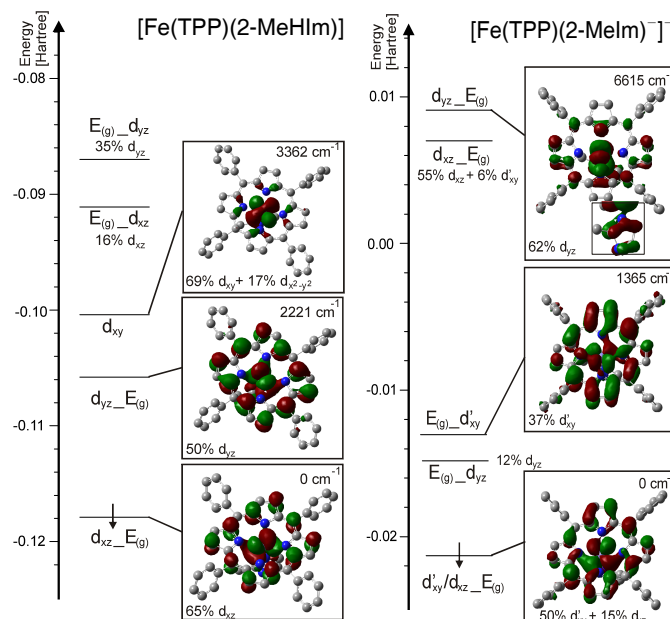


**Figure 6.** Frontier  $\beta$ -MO diagrams for  $[\text{Fe}(\text{TPP})(2\text{-MeHIm})]$  (left) and  $[\text{Fe}(\text{TPP})(2\text{-MeIm}^-)]^-$  (right) calculated with BP86/TZVP. The coordinate system has  $x$  and  $y$  located in the porphyrin plane, and  $z$  orthogonal to the porphyrin ring in the direction of the axial ligand.  $E(g)$  refers to the LUMO of the porphyrin (the index  $g$  is put in brackets because of the low symmetry of the porphyrin core). The nomenclature  $a.b$  indicates that orbital  $a$  interacts with  $b$  and that  $a$  has a larger contribution to the resulting MO. Reprinted with permission from *J. Am. Chem. Soc.* **2010**, *132*, 3737. Copyright 2010 American Chemical Society.

2.70 mm/s but that the sign is *opposite* to that of the globins (i.e. positive). It has long been postulated the histidine residue in HRP is strongly hydrogen bonded to a conserved aspartic acid that stabilizes higher oxidation states of iron and distinctly alters the chemical behavior of the peroxidases relative to the globins. The limit of a strong hydrogen bond would be the complete transfer of the hydrogen from histidine (or an imidazole). The crystal structures of heme proteins show that the appearance of a hydrogen bond to coordinated histidine is widespread. What is the effect of a coordinated, hydrogen-bonded imidazole on the electronic structure?

Several studies have shown that hydrogen bonding to imidazole increased the binding constant to form six-coordinate iron(III) complexes.<sup>38–40</sup> The hydrogen bond acceptors included imidazole itself, 1,10-phenanthroline, and substituted pyridines. A more recent study demonstrated that hydrogen bonding to a coordinated chloride in iron(III) porphyrinates could lead

to a spin state change.<sup>41</sup> In our first study of hydrogen bonding effects in iron(II) porphyrins, we obtained crystals that X-ray analysis showed contains two molecules of [Fe(TPP)(2-MeHIm)] and one additional molecule of 2-MeHIm.<sup>42</sup> The crystallization experiment was done in chlorobenzene with excess 2-MeHIm and 2,4,6-collidine. Interestingly, we obtained crystals of this same two-site species in the presence of several other hydrogen bond acceptors including 2-methylpyridine, triethylamine, and 2,2'-bipyridine whereas no crystalline products were isolated with DBU and proton sponge. The two molecules of [Fe(TPP)(2-MeHIm)] were found to have substantially different structures: site 1 looked very much like other imidazole derivatives whereas site 2 looked “imidazolate-like.” The “imidazolate-like” site is strongly hydrogen bonded to the solvate 2-methylimidazole with an N···N distance 2.824 Å. The structural parameters of this site are shown in the middle of Figure 7. The N–H of the coordinated imidazole was located in both X-ray and neutron diffraction studies and the 2-MeIm<sup>-</sup>/2-MeH<sub>2</sub>Im<sup>+</sup> case could be ruled out as the N–H distances is not perturbed substantially.<sup>42</sup> Mössbauer studies were attempted to define the effects of the hydrogen bonded and coordinated imidazole on the electronic structure. Measurements in zero field revealed a pair of quadrupole doublets with one doublet having quadrupole splitting values (2.40 mm/s, 4.2 K) consistent with values expected for imidazole derivatives and a second set of quadrupole splitting values (2.90 mm/s 4.2 K) close to, but somewhat smaller, than those seen for imidazolate. The value is very similar to that observed reduced HRP (2.70 mm/s, 4.2 K) with its known hydrogen-bonded histidine.<sup>37</sup>

Defining the sign of the quadrupole splitting of the two components requires the measurement in applied high magnetic field with attendant difficulties in deconvoluting the spectra. Simultaneous fits of 6 and 9 T measurements at various temperatures could lead to fits with a positive sign for the larger quadrupole doublet and a negative sign for the smaller quadrupole split doublet, i.e., imidazolate and imidazole value types. Although the fit was quite plausible, it is likely not the only possible fit to the data.

We also obtained several hydrogen-bonded species with 1,10-phenanthroline as the hydrogen bond acceptor.<sup>43</sup> In all crystalline species the porphyrin to 1,10-phen ratio is 1:1 and the two



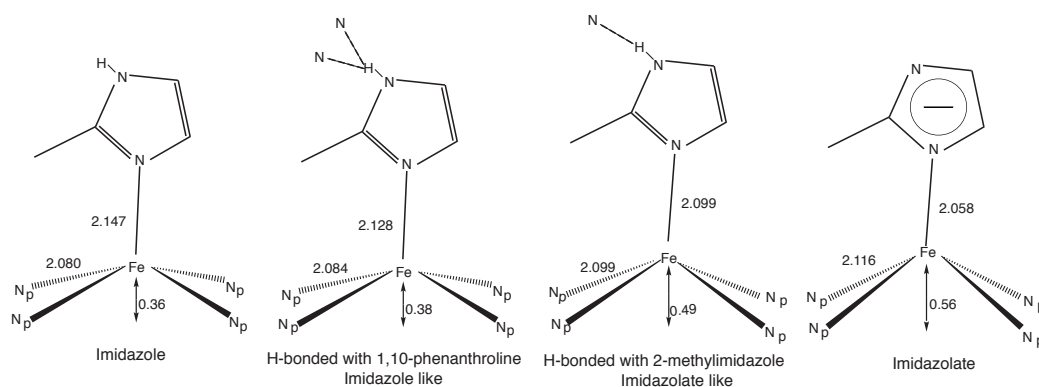


**Figure 7.** Diagrams illustrating the structural parameters of four possible groups of five-coordinate high-spin iron(II) porphyrinates. The number to the left in each diagram is the average Fe–N<sub>p</sub> distance, the middle number is the iron displacement from the four nitrogen plane and the top number is the value of the axial bond distance.

nitrogen atoms of the phenanthroline form two not quite equal hydrogen bonds. A total of five examples have been found in three different crystalline forms with the short N···N distance range of 2.95 to 3.00 Å and the longer N···N distance of 3.03 to 3.11 Å. Thus all structures are nearly equivalent. Mössbauer studies for both [Fe(TPP)(2-MeHim)]·1,10-phen and [Fe(OEP)(2-MeHim)]·1,10-phen have negative quadrupole splitting constants similar to imidazoles.

There is an interesting progression of coordination group geometry parameters as shown in Figure 7 that displays from left to right imidazole ligation, small hydrogen bonding effects, large hydrogen bonding effects, and complete deprotonation. Two parameters (Fe–N<sub>p</sub> bond distances and iron displacement,  $\Delta N_4$ ) increase in the series of four types from left to right, whereas the Fe–N<sub>Ax</sub> bond distance decreases. These must reflect the combined influences of the “size” of the iron(II) center and changes in the bonding with differing interactions at the N–H of the coordinated imidazole. However, the effects of hydrogen bonding on the electronic structure are somewhat difficult to predict with a relatively large gradation of possible effects from hydrogen bonding.

The thiolate-bound porphyrinate and hemoproteins appear to form a third group of high-spin iron derivatives as can be seen from the Mössbauer data. Since our main thrust in this work has been to understand the varying nature of imidazole-ligated hemes, we will not discuss

that system further.

## VI. CONCLUSIONS and OUTLOOK

There are clearly two distinct electronic states for high-spin iron porphyrinates that can be distinguished by structural differences and by physical methods, most prominently by the differences in the sign of the quadrupole splitting constant determined by Mössbauer spectroscopy. The end states are characterized by coordination of neutral imidazole or by imidazolate or other anions. There is a progression of modest changes in the molecular structure of the five-coordinate imidazole-ligated complexes as the the environment of the imidazole N–H is changed; the effects of hydrogen bonding can be seen. It is not completely clear where on this progression the electronic structure change would occur. The dichotomy of states has not been as well established in the hemes of the heme proteins. The possible biological functional significance for this difference has not been definitively established. The most likely scenario is that this distinction is reflected in the pathways for oxygen transport vs. oxygen utilization by the hemoproteins.

## ACKNOWLEDGEMENTS

WRS thanks the National Institutes of Health for support under Grant GM-38401.

## ABBREVIATIONS

TPP, tetraphenylporphyrin dianion; OEP, octaethylporphyrin dianion;  $TpOCH_3PP$ , tetra*para*-methoxyphenylporphyrin dianion; TTP, tetratolylporphyrin dianion;  $T_{piv}PP$ , picket fence porphyrin dianion; 2-MeHIm, 2-methylimidazole;  $2-MeIm^-$ , 2-methylimidazolate; 1,2-Me<sub>2</sub>Im, 1,2-dimethylimidazole; Hdmpz, 3,5-dimethylpyrazole.

## BIOGRAPHIES

**Chuanjiang Hu** received his B.S. (1995), and Ph.D. (2000) from Nanjing University working with Qingjin Meng. He was a Postdoctoral Fellow at the University of Florence with Dante Gatteschi, San Jose State University with Paul S. Wagenknecht and University of Notre Dame with W. Robert Scheidt from 2001 to 2006, a research assistant professor at University of Notre Dame (2006–2008). He has been Professor of Chemistry at Soochow University since 2008. His research interests are in inorganic, coordination and supramolecular chemistry. His research activity is focused on chiral recognition of biological molecules, biomimetic models of metalloenzymes and heme proteins, and porphyrin-based electronic, photonic and magnetic materials.



**Charles E. Schulz** is Professor of Physics at Knox College. He earned his Ph.D. in Physics from the University of Illinois at Urbana/Champaign in 1979 under Prof. Peter Debrunner, and was a postdoctoral associate in Molecular Biophysics and Biochemistry at Yale (1979-1981) with Prof. Joseph Coleman. His research activity is focused on Mössbauer characterization of metalloproteins and model compounds. He is the author of numerous publications in highly-ranked journals, including *Angewandte Chemie*, *Journal of the American Chemical Society*, and *Journal of Chemical Physics*.



**W. Robert Scheidt** received his B.S. from the University of Missouri-Columbia and his Ph.D. from the University of Michigan. After a postdoctoral (1968-1970) with Prof. J. L. Hoard at Cornell, he joined the faculty at the University of Notre Dame, where he rose through the ranks and is now the Wm. K. Warren Professor of Chemistry and Biochemistry. His research interests in metalloporphyrin chemistry include structural trends and the relationship between molecular structure and physical observables including magnetic and spectroscopic properties. He is the author of over 350 publications.



**Table 1.** Mössbauer Parameters for Five-Coordinate, High-Spin Iron(II) porphyrinates and proteins at 4.2 K

Complex	$\Delta E_Q^a$	$\delta_{\text{Fe}}^a$	$\eta$	ref.
[Fe(TPP)(2-MeHIm)(2-fold)]	-2.28	0.93	0.8	18
[Fe(TPP)(1,2-Me <sub>2</sub> Im)]	-2.16	0.92	0.7	18
[Fe(TPP)(2-MeHIm)]	-2.40	0.92	0.8	13
[Fe(T <sub>p</sub> OCH <sub>3</sub> PP)(1,2-Me <sub>2</sub> Im)]	-2.44	0.95	0.6	14
[Fe(T <sub>p</sub> OCH <sub>3</sub> PP)(2-MeHIm)]	-2.18	0.94	0.58	14
[Fe(TPP)(1,2-Me <sub>2</sub> Im)]	-1.93	0.92	0.53	14
[Fe(TTP)(1,2-Me <sub>2</sub> Im)]	-2.06	0.86	0.58	14
[Fe(OEP)(1,2-Me <sub>2</sub> Im)]	-2.23	0.92	0.50	15
[Fe(OEP)(2-MeHIm)]	-1.96	0.90	0.48	15
[Fe((Piv <sub>2</sub> C <sub>8</sub> P)(1-MeIm)]	-2.3 <sup>b</sup>	0.88	-	16
[Fe(TPP)(Hdmpz)]	-2.54	0.91	0.74	20
[Fe(TPP)(2-MeHIm)] <sub>2</sub> ·(2-MeHIm) (site 1) <sup>c</sup>	-2.40	0.92	0.90	42
[Fe(TPP)(2-MeHIm)] <sub>2</sub> ·(2-MeHIm) (site 2) <sup>d</sup>	+2.94	0.97	0.71	42
[Fe(TPP)(2-MeHIm)]·(1,10-phen)	-2.12 <sup>b,e</sup>	0.90		43
[Fe(OEP)(2-MeHIm)]·(1,10-phen)	-1.93	0.94	0.76	43
[Fe(OEP)(2-MeIm <sup>-</sup> )]	+3.71	1.00	0.22	33
[Fe(TPP)(2-MeIm <sup>-</sup> )]	+3.60	1.00	0.02	33
[Fe(T <sub>piv</sub> PP)(2-MeIm)] <sup>-</sup>	+3.51 <sup>f,g</sup>	0.97		32
[Fe(TPP)(OC <sub>6</sub> H <sub>5</sub> )] <sup>-</sup>	+4.01	1.03	0.25	25
[Fe(T <sub>piv</sub> PP)(O <sub>2</sub> CCH <sub>3</sub> )] <sup>-</sup>	+4.25	1.05	0.30	27
[Fe(T <sub>piv</sub> PP)Cl] <sup>-</sup>	+4.36 <sup>f,g</sup>	1.01		26
[Fe(T <sub>piv</sub> PP)(OCH <sub>3</sub> )] <sup>-</sup>	+3.67 <sup>f</sup>	1.03		28
[Fe(T <sub>piv</sub> P)(OC <sub>6</sub> H <sub>5</sub> )] <sup>-</sup>	+3.90 <sup>f</sup>	1.06		28
[Fe(T <sub>piv</sub> PP)ONO <sub>2</sub> ] <sup>-</sup>	+3.59 <sup>f,g</sup>	0.98		29
[Fe(T <sub>piv</sub> P)(SC <sub>6</sub> HF <sub>4</sub> )] [NaC <sub>12</sub> H <sub>24</sub> O <sub>6</sub> ]	+2.38 <sup>f</sup>	0.84		27
[Fe(T <sub>piv</sub> PP)(SC <sub>6</sub> HF <sub>4</sub> )] [NaC <sub>22</sub> 22]	+2.38 <sup>f</sup>	0.83		26
[Fe(T <sub>piv</sub> PP)(SC <sub>2</sub> H <sub>5</sub> )] <sup>-</sup>	+2.18	0.83	0.80	27
deoxyHb	-2.40	0.92	0.7	18
deoxyMb	-2.22	0.92	0.7	18
Reduced HRP	+2.70	0.90		37
P-460	+4.21	0.96		30
cyt P-450	+2.42	0.82	0.8	44
CPO	+2.50	0.85	1.0	37

<sup>a</sup> mm/s. <sup>b</sup> Sign not determined experimentally, presumed negative.

<sup>c</sup> No hydrogen bond. <sup>d</sup> Hydrogen bond to 2-MeHIm solvate. <sup>e</sup> 20K.

<sup>f</sup> Sign not determined experimentally, presumed positive. <sup>g</sup> 77K.

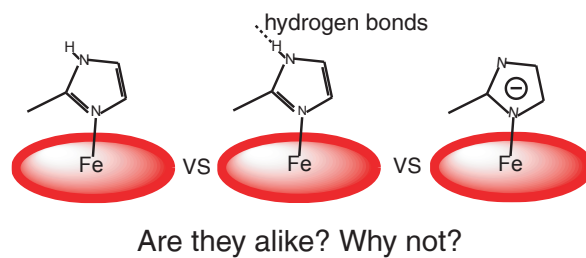
## References and Notes

- 1 J. Peisach, W. E. Blumberg and A. Adler, *Ann. N.Y. Acad. Sci.*, 1973, **206**, 310–327.
- 2 J. S. Valentine, R. P. Sheridan, L. C. Allen and P. C. Kahn, *Proc. Nat. Acad. Sci.*, 1979, **76**, 1009–1013.
- 3 G. I. Berglund, G. H. Carlsson, A. T. Smith, H. Szöke, A. Henriksen and J. Hajdu, *Nature*, 2002, **417**, 4863–4868.
- 4 C. M. Casadei, A. Gumiero, C. L. Metcalfe, E. J. Murphy, J. Basran, M. G. Concilio, S. C. M. Teixeira, T. E. Schrader, A. J. Fielding, A. Ostermann, M. P. Blakeley, E. L. Raven and P. C. E. Moody, *Science*, 2014, **345**, 193–197.
- 5 J. P. Collman and C. A. Reed, *J. Am. Chem. Soc.*, 1973, **95**, 2048–2049.
- 6 K. Rachlewicz, L. Latos-Grzążyński and E. Vogel, *Inorg. Chem.*, 2000, **39**, 3247–3251.
- 7 A. M. Stolzenberg, S. H. Strauss and R. H. Holm, *J. Am. Chem. Soc.*, 1981, **103**, 4763–4778.
- 8 J. P. Collman, *Acc. Chem. Res.*, 1977, **10**, 265–272.
- 9 J. P. Collman, N. Kim, J. L. Hoard, G. Lang, L. J. Radonovich and C. A. Reed, *Abstracts of Papers*; 167th National Meeting of the American Chemical Society; Los Angeles, CA, April 1974; American Chemical Society: Washington, D. C., INOR 29.
- 10 J. L. Hoard and W. R. Scheidt, *Proc. Natl. Acad. Sci. U.S.A.*, 1973, **70**, 3919–3922.
- 11 W. R. Scheidt and C. A. Reed, *Chem. Rev.*, 1981, **81**, 543–555
- 12 We distinguish the two forms of [Fe(TPP)(2-MeHIm)] by appending the suffix (twofold) to the Reed, Collman prep.
- 13 M. K. Ellison, C. E. Schulz and W. R. Scheidt, *Inorg. Chem.*, 2002, **41**, 2173–2181.
- 14 C. Hu, A. Roth, M. K. Ellison, J. An, C. M. Ellis, C. E. Schulz and W. R. Scheidt, *J. Am. Chem. Soc.*, 2005, **127**, 5675–5688.
- 15 C. Hu, J. An, B. C. Noll, C. E. Schulz and W. R. Scheidt, *Inorg. Chem.*, 2006, **45**, 4177–4185.
- 16 M. Momenteau, W. R. Scheidt, C. W. Eigenbrot and C. A. Reed, *J. Am. Chem. Soc.*, 1988, **110**, 1207–1215.

- 17 T. A. Kent, K. Spartalian, G. Lang, T. Yonetani, C. A. Reed and J. P. Collman, *Biochim. Biophys. Acta* (BBA)-Protein Structure, 1979, **580**, 245–258.
- 18 T. A. Kent, K. Spartalian and G. Lang, *J. Chem. Phys.*, 1979, **71**, 4899–4898.
- 19 C. Hu, C. D. Sulok, F. Paulat, N. Lehnert, A. I. Twigg, M. P. Hendrich, C. E. Schulz and W. R. Scheidt, *J. Am. Chem. Soc.*, 2010, **132**, 3737–3750.
- 20 C. Hu, B. C. Noll, C. E. Schulz and W. R. Scheidt, *Inorg. Chem.*, 2010, **49**, 10984–10991.
- 21 M. Schappacher, L. Ricard, R. Weiss, R. Montiel-Montoya, U. Gonser, E. Bill and A. X. Trautwein, *Inorg. Chim. Acta*, 1983, **78**, L9-L12.
- 22 J. Silver and B. Lukas, *Inorg. Chim. Acta*, 1983, **80**, 107–113.
- 23 J. Silver, B. Lukas and G. Al-Jaff, *Inorg. Chim. Acta* 1984, **91**, 125–128.
- 24 H. Nasri, J. Fischer, R. Weiss, E. Bill, and A. Trautwein, *J. Am. Chem. Soc.*, 1987, **109**, 2549–2550.
- 25 B. A. Shaevitz, G. Lang and C. A. Reed, *Inorg. Chem.*, 1988, **27**, 4607–4613.
- 26 M. Schappacher, L. Ricard, J. Fischer, R. Weiss, R. Montiel-Montoya, E. Bill and A. X. Trautwein, *Inorg. Chem.*, 1989, **28**, 4639–4645.
- 27 E. L. Bominaar, X. Q. Ding, A. Gismelseed, E. Bill, H. Winkler, A. X. Trautwein, H. Nasri, J. Fischer and R. Weiss, *Inorg. Chem.*, 1992, **31**, 1845–1854.
- 28 H. Nasri, J. Fischer, R. Weiss, E. Bill and A. X. Trautwein, *J. Am. Chem. Soc.*, 1987, **109**, 2549–2550.
- 29 H. Nasri, M. K. Ellison, B. Shaevitz, G. P. Gupta and W. R. Scheidt, *Inorg. Chem.*, 2006, **45**, 5284–5290.
- 30 K. K. Anderson, T. A. Kent, J. D. Lipscomb, A. B. Hooper and E. Munck, *J. Biol. Chem.*, 1984, **259**, 6833–6840.
- 31 P. Debrunner, In *Iron Porphyrins Part 3*; A. B. P Lever and H. B. Gray, Eds.; VCH Publishers Inc.; New York, 1983; Chapter 2.
- 32 D. Mandon, F. Ott-Woelfel, J. Fischer, R. Weiss, E. Bill and A. X. Trautwein, *Inorg. Chem.*, 1990, **29**, 2442–2447.
- 33 C. Hu, B. C. Noll, C. E. Schulz and W. R. Scheidt, *J. Am. Chem. Soc.*, 2005, **127**, 15018–15019.

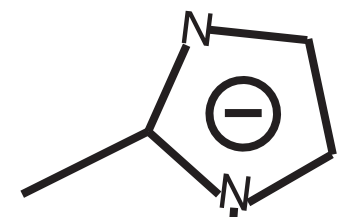
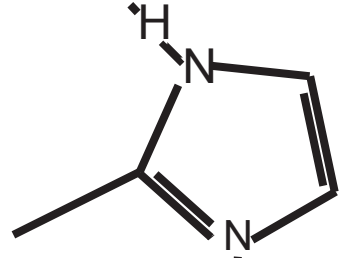
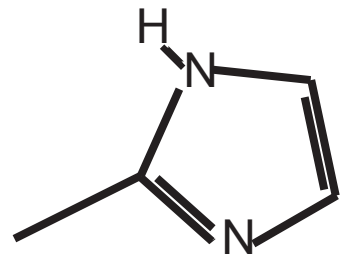
- 34 W. R. Scheidt, S. M. Durbin and J. T. Sage, *J. Inorg. Biochem.*, 2005, **99**, 60–71.
- 35 C. Hu, A. Barabanschikov, M. K. Ellison, J. Zhao, E. E. Alp, W. Sturhahn, M. Z. Zgierski, J. T. Sage and W. R. Scheidt, *Inorg. Chem.*, 2012, **51**, 1359–1370.
- 36 C. Hu, Q. Peng, N. J. Silvernail, A. Barabanschikov, J. Zhao, E. E. Alp, W. Sturhahn, J. T. Sage and W. R. Scheidt, *Inorg. Chem.*, 2013, **52**, 3170–3177.
- 37 P. M. Champion, I. R. Chiang, E. Munck, P. Debrunner and L. P. Hager, *Biochemistry*, 1975, **14**, 4159–4166.
- 38 C. L. Coyle, P. A. Rafson and E. H. Abbott, *Inorg. Chem.*, 1973, **12**, 2007–2010.
- 39 F. A. Walker, M. W. Lo and M. T. Ree, *J. Am. Chem. Soc.*, 1976, **98**, 5552–5560.
- 40 A.L. Balch, J. J. Watkins, and D. J. Doonan, *Inorg. Chem.*, 1979, **18**, 1228–1231.
- 41 D. Sahoo, M. G. Quesne, S. P. de Visser and S. P. Rath. *Angew. Chem., Int. Ed. Engl.* 2015 **54**, 4796–4800.
- 42 C. Hu, B. C. Noll, P. M. B. Piccoli, A. J. Schultz, C. E. Schulz and W. R. Scheidt, *J. Am. Chem., Soc.* 2008, **130**, 3127–3136.
- 43 C. Hu, B. C. Noll, C. E. Schulz and W. R. Scheidt, *Inorg. Chem.*, 2008, **47**, 8884–8895.
- 44 P. M. Champion, J. D. Lipscomb, E. Munck, P. Debrunner and I. C. Gunsalus, *Biochemistry*, 1975, **14**, 4151–4158.





High spin iron(II) porphyrinates ligated by imidazole, hydrogen-bonded imidazole, and imidazolate are found to display two distinct electronic structures.

hydrogen bonds



Fe

VS

Fe

VS

Fe

Are they alike? Why not?